JACS
JOURNAL OF THE AMERICAN CHEMICAL SOCIETY
Communication
pubs.acs.org/JACS

Specific Enrichment of Phosphoproteins Using Functionalized Multivalent Nanoparticles

Leekyoung Hwang,[†] Serife Ayaz-Guner,[‡] Zachery R. Gregorich,[‡,§] Wenxuan Cai,[‡,§] Santosh G. Valeja,[‡] Song Jin,*[,†] and Ying Ge*[,†,‡,§,∥]

[†]Department of Chemistry, [‡]Department of Cell and Regenerative Biology, [§]Molecular and Cellular Pharmacology Program, and [∥]Human Proteomics Program, University of Wisconsin−Madison, Madison, Wisconsin 53719, United States

Supporting Information

ABSTRACT: Analysis of protein phosphorylation remains a significant challenge due to the low abundance of phosphoproteins and the low stoichiometry of phosphorylation, which requires effective enrichment of phosphoproteins. Here we have developed superparamagnetic nanoparticles (NPs) whose surface is functionalized by multivalent ligand molecules that specifically bind to the phosphate groups on any phosphoproteins. These NPs enrich phosphoproteins from complex cell and tissue lysates with high specificity as confirmed by SDS-PAGE analysis with a phosphoprotein-specific stain and mass spectrometry analysis of the enriched phosphoproteins. This method enables universal and effective capture, enrichment, and detection of intact phosphoproteins toward a comprehensive analysis of the phosphoproteome.

Protein phosphorylation, one of the most common and important post-translational modifications, plays a pivotal role in the control of many biological processes, including cell growth, division, and signaling;[1] and aberrant phosphorylation has been implicated in the pathogenesis of human diseases.[2] Therefore, a comprehensive analysis of phosphoproteins is essential for understanding cellular biology and disease mechanisms. However, analysis of protein phosphorylation is challenging mainly due to the low abundance of phosphoproteins and the low stoichiometry of phosphorylation.[3] Mass spectrometry (MS) has become the method of choice for the analysis of protein phosphorylation,[3,4] but it is nearly impossible to analyze phosphoproteins directly from the complex proteome by MS without a specific enrichment procedure.

In the past decade, a plethora of methods have been developed for the enrichment and MS analysis of phosphopeptides from protein digests.[3−5] The digestion of each protein into hundreds of peptides significantly increases the overall complexity. In contrast, enriched intact phosphoproteins can be directly analyzed by top-down MS for comprehensive characterization of phosphorylation.[2b,6] However, very few methods[7] are available for the enrichment of phosphoproteins and each has different major drawbacks. Although phospho-specific anti-phosphotyrosine antibodies have high affinity,[7a] the enrichment of phosphoserine/threonine containing proteins (which represent >99% of all phosphoproteins)[3,4] remains a challenge due to the low affinity and specificity of phospho-Ser/Thr antibodies.[4a,7a] The enrichment strategies employing immobilized metal ion affinity chromatography (IMAC)[7a,c] can enrich proteins with phosphorylated Ser, Thr, and Tyr residues without bias; however, they have low specificity, efficiency, and poor reproducibility.[8] Thus, the effective capture and universal enrichment of phosphoproteins from complex mixtures remains a significant challenge. Herein, we have designed and synthesized functionalized multivalent superparamagnetic nanoparticles (NPs) to universally and effectively enrich phosphoproteins from complex mixtures. The effectiveness of NP-enabled

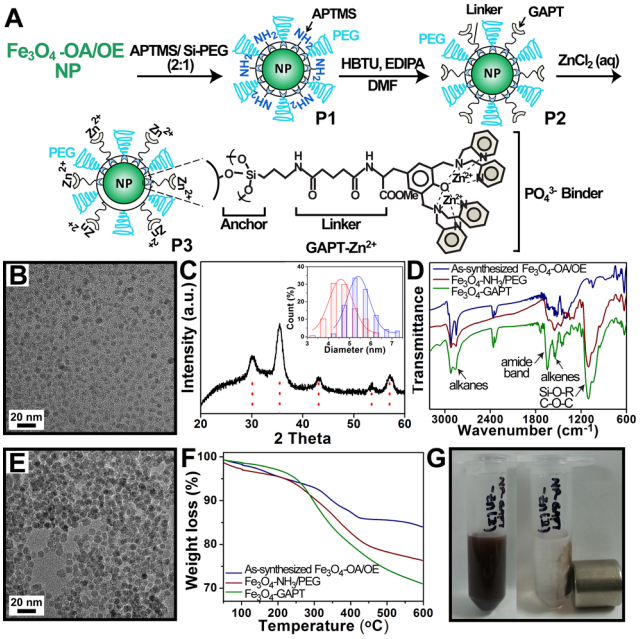

Figure 1. (A) Schematic illustration of the synthesis and functionalization of Fe_3O_4 NPs. GAPT-Zn chelate groups have strong binding to phosphate groups. Molecules and NPs are not drawn to scale. (B) TEM image and (C) PXRD pattern of as-synthesized Fe_3O_4-OA/OE NPs. Inset shows the size distributions of the Fe_3O_4-OA/OE (red) and Fe_3O_4-GAPT-Zn (blue) (D) FTIR of Fe_3O_4-OA/OE (blue), Fe_3O_4-NH_3^+/PEG (red), and Fe_3O_4-GAPT (green) NPs. (E) TEM image of the functionalized Fe_3O_4-GAPT-Zn NPs. (F) TGA analysis of Fe_3O_4-OA/OE(blue), APTMS and Si-PEG (red), and GAPT coupled to APTMS (green). (G) Functionalized Fe_3O_4-GAPT-Zn NPs well-dispersed (left) and collected by a magnet (right) in aqueous solutions.

Received: November 18, 2014
Published: February 5, 2015

DOI: 10.1021/ja511833y
J. Am. Chem. Soc. 2015, 137, 2432−2435

phosphoprotein enrichment from complex cell and tissue lysates was demonstrated by SDS-PAGE analysis with a phosphoprotein-specific stain, and furthermore by top-down MS analyses of the enriched phosphoproteins (Figure S1).

In our approach, we utilized superparamagnetic iron oxide (magnetite, Fe_3O_4) NPs with a small diameter ranging 4−6 nm (Figure 1). The small size of the NPs gives them a high surface-to-volume ratio, which allows for easy modification of the NPs' surface with multivalent ligand molecules properly designed to have a specific interaction with target proteins.[9] Furthermore, the size of NPs is comparable to the size of proteins, therefore enabling the NPs to (i) penetrate better in protein mixtures, leading to a higher binding rate; (ii) reduce the probability that proteins are denatured; and (iii) have good solubility.[9b,c,10] Furthermore, Fe_3O_4 NPs of this small size (below 20 nm) are superparamagnetic;[11] therefore, unlike bulky micron-sized magnetic beads, the NPs are not spontaneously magnetic without external magnetic field. This property prevents the NPs from aggregating by themselves due to mutual magnetic attraction, but enables them to aggregate and precipitate readily under applied magnetic fields. Crucial to the specific capture, enrichment, and release of the phosphoproteins is the use of a dinuclear Zn (II)-dipicolylamine (Zn-DPA) complex as an affinity ligand to specifically bind to the phosphate groups (Figure 1A). The Zn-DPA coordination complex has a vacancy on two Zn metal ions that the phosphate dianion ($ROPO_3^{2-}$) can access to form the complex $ROPO_3^{2-}$-$(2Zn\text{-}DPA)^{3+}$, and therefore is known to exhibit a high affinity toward anionic phosphorylated chemical species (against SO_4^{2-}, CH_3COO^-, and Cl^-) in aqueous solution at a neutral pH.[12] Therefore, acrylamides containing copolymerized M^{2+}-DPA complexes (so-called "phos-tag") have been used for phosphate-affinity gel electrophoresis and visualization of proteins with phosphorylated Ser, Thr, and Tyr residues without bias.[12]

We synthesized Fe_3O_4 NPs functionalized with Zn-DPA ligands that are linked via glutaric acid (hereafter referred to as GAPT), as illustrated in Figure 1A. First, oleic acid (OA) and oleylamine (OE)-capped Fe_3O_4 NPs were synthesized as reported previously (see SI for detailed procedures).[13] Transmission electron microscopy (TEM) imaging (Figure 1B) revealed that the size of as-synthesized Fe_3O_4-OA/OE NPs was 4.6 ± 0.7 nm (red size distribution histogram in Figure 1C inset). Powder X-ray diffraction (PXRD) confirmed the Fe_3O_4 NPs to be magnetite (Figure 1C). Next, the hydrophobic OA and OE ligands on these intermediate Fe_3O_4 NPs were exchanged with 3-aminopropyl trimethoxysilane (APTMS) and 2-methoxy (polyethyleneoxy) propyl trimethoxysilane (hereafter referred to as Si-PEG), to produce Fe_3O_4-NH_3^+/PEG (Figure 1A, P1).[14] These PEG groups, which contain a polyethyleneoxy moiety, decrease nonspecific interactions between proteins and the NPs and improve the solubility of the NPs in aqueous buffers.[15] Subsequently, the Zn-chelating ligand molecules, GAPT, which were synthesized following a previous report,[16] were coupled to the free amino groups of the APTMS molecules on the NPs. Finally, the Fe_3O_4-GAPT NPs (Figure 1A, P2) were activated with 10 mM $ZnCl_2$ (aq) to generate Fe_3O_4-GAPT-Zn NPs (Figure 1A, P3). TEM showed that the average size of Fe_3O_4-GAPT-Zn NPs increased to 5.4 ± 0.6 nm (blue histogram in Figure 1C inset) except that its aggregation was slightly increased (Figure 1E). Fourier transform infrared spectroscopy (FTIR) was used to confirm the proper functionalization of NPs with the ligand molecules. The broad and strong band around 1022 cm^{-1} and peaks around 1200 cm^{-1} of Fe_3O_4-NH_3/PEG NPs indicated

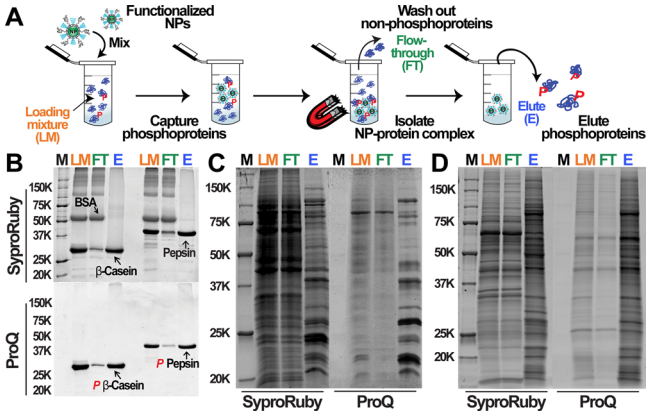

Figure 2. (A) Workflow of the capture and enrichment strategy using the functionalized NPs. (B) SDS-PAGE analysis with Sypro Ruby (top) and Pro-Q Diamond (bottom) staining confirmed the highly specific enrichment of phosphoproteins (β-casein and pepsin) from standard protein mixtures containing non-phosphoprotein (BSA). M, molecular markers; LM, loading mixture before enrichment; FT, flow-through; and E, elution after enrichment. (C,D) Global enrichment of phosphoproteins from (C) HEK 293 cell lysate (equal amount loading, 15 μg) and (D) swine heart tissue extract (equal amount loading, 10 μg) as demonstrated by SDS-PAGE analysis with Sypro Ruby (left side) and Pro-Q Diamond staining (right side).

the existence of Si-O-R and C-O-C, EO CH_2,[14a] and the sharp peak around 1630 $cm^{-1}$of Fe_3O_4-GAPT NPs proved the existence of the amide bond (Figure 1D). In addition, thermogravimetric analysis (TGA) of the as-synthesized Fe_3O_4, Fe_3O_4-NH_3^+/PEG, and Fe_3O_4-GAPT NPs showed a different weight loss (%) for each of the surface-modified NPs that was commensurate with the corresponding ligand molecules (Figure 1F). After activating Fe_3O_4-GAPT NPs with Zn ions, we used X-ray photon spectroscopy (XPS) to observe the characteristic Zn 2p peak at 1020 eV (Figure S2) and confirm the presence of Zn on the NP surface. The resulting NPs can be dispersed in aqueous solution and gathered using a magnet (Figure 1G).

Next, we performed phosphoprotein enrichment experiments using the functionalized Fe_3O_4-GAPT-Zn NPs (Figure 2A) as follows: (1) mixing and agitating the protein mixture with the NPs, (2) removing the unbound non-phosphoproteins as flow-through, and (3) elution of the phosphoproteins. We tested the phosphoprotein enrichment from standard protein mixtures containing either β-casein or pepsin (both of which are phosphoproteins) and bovine serum albumin (BSA, a non-phosphoprotein) in the same mass-to-volume ratio. The best enrichment results were obtained using a buffer solution containing 50 mM HEPES and 150 mM NaCl (pH 7.7) for binding and subsequent washing, and a buffer containing 100 mM Na_2HPO_4 and 200 mM NaCl (pH adjusted to 7.3 with HCl) for elution. The large excess of phosphate ions in the elution buffer out-competes the phosphate groups on the captured phosphoproteins for binding to the NPs, thereby releasing the phosphoproteins.

We used SDS-PAGE to demonstrate the selective enrichment of phosphoproteins by the functionalized NPs (Figure 2B). The gel was first stained by Pro-Q Diamond fluorescent dye to visualize phosphoproteins and then by Sypro Ruby dye to observe the profile of total proteins (including both non-phosphoproteins and phosphoproteins) in the gel. After enrichment, in the elution solutions the bands corresponding to β-casein and pepsin were far more prominent, whereas the

DOI: 10.1021/ja511833y
J. Am. Chem. Soc. 2015, 137, 2432−2435

non-phosphoprotein, BSA, was nearly absent (Figure 2B, top). In contrast, the flow-through solution contained significantly higher amount of BSA. Moreover, Pro-Q Diamond stained only β-casein or pepsin, not BSA (Figure 2B, bottom), confirming that the eluted β-casein and pepsin are indeed phosphoproteins. These results show that the Fe_3O_4-GAPT-Zn NPs can selectively bind to phosphoproteins in mixtures containing non-phosphoproteins. To confirm the importance of the metal-ion chelating group GAPT-Zn for the specific binding to phosphate groups, we compared protein binding using three different control NPs: (1) Fe_3O_4-GAPT NPs that were not activated by Zn^{2+}; (2) Fe_3O_4-NH_3^+/PEG NPs that were functionalized with positively charged ligands, but without GAPT ligands; and (3) Fe_3O_4-PEG NPs that were functionalized only with PEG groups. All of the control NPs showed poor affinity or reversible binding toward phosphoproteins in the same enrichment experiments with the standard protein mixtures (Figure S3). These control experiments unequivocally confirmed that the specific binding of phosphoproteins occurs via interactions between the phosphate group and the GAPT-Zn ligand complex on the surface of the Fe_3O_4-GAPT-Zn NPs.

To further evaluate the specificity of the phosphoprotein enrichment, we systematically increased the mass ratio of BSA:β-casein from 9:1 to 99:1 while holding the amount of β-casein constant at 200 μg. The β-casein was clearly enriched even in the mixture containing an overwhelming amount of BSA (BSA:β-casein = 99:1) (see Figure S4A,B). We determined the percentage of protein recovery and the enrichment factor (defined as the gain in the relative ratio of the phosphoprotein to non-phosphoprotein) to assess the performance of phosphoprotein enrichment (Figure S4C,D). For a mixture of 99:1 BSA to β-casein, the enrichment factor was over 140-fold (Figure S4D), which could almost be considered "purification" of phosphoproteins. The enrichment performance of Fe_3O_4-GAPT-Zn NPs was also compared with an IMAC-based phosphoprotein enrichment kit (Thermo). For the same enrichment experiment of a mixture of 99:1 BSA to β-casein, our NPs showed significantly reduced nonspecific binding and greatly outperformed this IMAC-based material (Figure S5).

We further assessed the enrichment of phosphoproteins from human embryonic kidney (HEK) 293 cell lysate (Figure 2C) and swine heart tissue extract (Figure 2D), two highly complex mixtures, using the Fe_3O_4-GAPT-Zn NPs. We loaded equal amounts of proteins before and after enrichment on the SDS-PAGE gel, stained with Pro-Q Diamond first, destained, and restained with Sypro Ruby (for total protein detection). Despite the equal amount loading as confirmed by the similar total intensities of the loading mixture before enrichment (LM), flow-through (FT), and the elution after enrichment (E) lanes stained by Sypro Ruby, the Pro-Q Diamond-stained LM and FT lanes showed significantly lower intensity than the E lane, suggesting that most of the proteins in the LM and FT are non-phosphoproteins. Furthermore, the banding patterns of the E lane stained with both Pro-Q Diamond and Sypro Ruby are highly similar, in contrast to the LM and FT lanes which are very different between the Pro-Q Diamond and Sypro Ruby stains, indicating the enriched proteins are predominantly phosphoproteins. These results clearly indicate that the Fe_3O_4-GAPT-Zn NPs can specifically and effectively enrich phosphoproteins from complex biological samples with high affinity and efficiency.

To demonstrate our NP enrichment strategy is compatible with top-down MS, we have examined the intact proteins present in the complex swine heart tissue extracts before and after enrichment by LC-MS. The LM and E solutions from swine heart tissue extract without digestion were desalted, concentrated, and separated by reverse phase chromatography. Subsequent MS analysis of the LM revealed that most of the detected proteins are highly abundant blood proteins, such as hemoglobin subunit α (see Figure S6) or β, and myoglobin. However, these blood proteins were either not detected or dramatically decreased by MS in the E solution (Figure S7A). This suggests that these highly abundant non-phosphoproteins were not captured by the NPs and, consequently, were removed during the washing step.

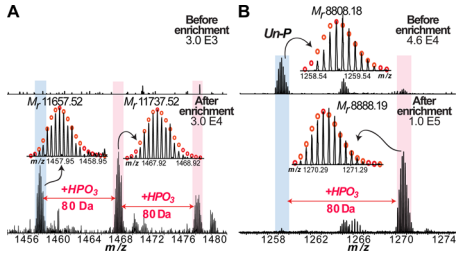

Figure 3. Representative intact protein MS spectra, before and after enrichment, confirming the highly specific enrichment of phosphoprotein from a swine heart tissue extract. (A) Low abundance phosphoprotein that is not detectable before enrichment (top) is detected after enrichment (bottom). (B) Phosphoprotein with very low phosphorylation occupancy that the unphosphorylated form (*Un-P*) is predominant before the enrichment but the phosphorylated form (*+P*) becomes dominant after the enrichment. M_r = most abundant molecular weight. $+HPO_3$, the covalent addition of a phosphate group (+80 Da).

Importantly, the top-down MS data clearly showed that phosphoproteins in swine heart tissue extracts were enriched by the Fe_3O_4-GAPT-Zn NPs, even in the presence of highly abundant blood proteins (vide supra). Many of the detected phosphoproteins have very low abundance in comparison to non-phosphoproteins and/or low stoichiometry (low phosphorylation occupancy) in the pre-enrichment samples; however, these phosphoproteins were significantly enriched in the post-enrichment samples, some with more than one phosphorylation detected for the same protein (mass increases of multiples of 80 Da) (Figures 3 and S7B). As a representative example, after enrichment, a protein with M_r 11 657.52 (M_r, most abundant molecular weight) was detected by top-down MS together with two additional peaks with 80 Da mass increases (labeled $+HPO_3$) (Figure 3A, bottom), which correspond to multiple phosphorylated forms of the protein. However, none of these peaks were detected in the MS before enrichment (Figure 3A, top) implying they are all phosphorylated protein forms that have low abundance. Another representative MS of the original protein mixture before enrichment displayed a protein with M_r 8808.18 (Figure 3B, top, labeled *Un-P*). After enrichment, a protein with M_r 8888.19 with a mass increase of 80 Da was detected in the MS instead (Figure 3B, bottom, labeled *+P*). This clearly shows that the relative abundance of the phosphorylated species (M_r 8888.19) is significantly increased compared to the non-phosphorylated species (M_r 8808.18) after enrichment. It should also be noted that a few Zn^{2+}-binding proteins, such as a parathymosin-like protein[17] (Figure S8), were also detected in the E fractions due to its high affinity to GAPT-Zn ligands on the NPs. Thus, top-down MS analysis confirmed that the number and amount of phosphoproteins in the E fraction were significantly increased compared to the LM, which was dominated by overwhelmingly abundant blood proteins. The

DOI: 10.1021/ja511833y
J. Am. Chem. Soc. 2015, 137, 2432−2435

fact that no high-mass phosphoproteins were identified in this top-down MS study is mostly likely due to the exponential decay in the signal-to-noise ratio that occurs with increasing mass in high-resolution MS[18a] and the use of Q-Exactive mass spectrometer, which is not optimized for high-mass protein detection.[18b] However, high-mass proteins (20−150 kDa) were clearly detected by SDS-gel analyses of the E fractions after phosphoenrichment from HEK293 cell lysates (Figure 2C) and swine heart tissue extracts (Figure 2D). This confirms that high-mass phosphoproteins were indeed enriched by the NPs.

To recapitulate, we have developed superparamagnetic NPs that are functionalized with multivalent ligands to capture and enrich intact phosphoproteins with high specificity and efficacy. Such functionalized NPs can have many advantages for phosphoprotein enrichment: (a) They have a high surface area per volume,[9,10] as a result of the small NP size. The NP diameter of ∼5 nm (Figure 1C) corresponds to a surface area of >200 m^2/g (see calculation in Table S1), which translates into high ligand density. (b) NPs have comparable nanometer size to proteins and can be well-dispersed in aqueous solution (as shown in Figure 1G). This gives NPs similar kinetics to proteins and allow them to intermingle well with proteins as demonstrated previously,[9b,c,10] therefore allowing for effective capture of phosphoproteins. (c) The NPs developed here have multiple flexible binding sites (see an estimate in Table S2) packed in a small dimension comparable to the size of proteins; this multivalency effect[19] can increase the overall binding affinity and ensure the efficient capture of low concentration phosphoproteins. (d) NPs modified with GAPT-Zn complex enrich all phosphoproteins regardless whether it is Ser, Thr, or Tyr phosphorylation[12c] to allow a global and comprehensive analysis of phosphoproteins. (e) Unlike conventional bottom-up approach which requires digestion of proteins into peptides, NPs capture intact phosphoproteins in physiological conditions directly and reversibly. Circular dichroism measurements revealed that the enriched protein maintained the same conformation as the original one (Figure S9). The enriched intact phosphoproteins can be analyzed by conventional biochemical methods such as Western blotting and top-down MS technologies for comprehensive phosphoprotein characterization.[2b,6] (f) In comparison to the development and production of new antibodies for capturing phosphoproteins, which are labor intensive, expensive, and difficult to scale up, the synthesis of NPs is simpler, faster, and more scalable. These advantages of the NP approach have enabled us to demonstrate the specific enrichment of phosphoproteins from complex cell and tissue lysates, as confirmed by SDS-PAGE analysis with phosphospecific stain and top-down MS analysis. This simple, effective, and universal nanoparticle-based phosphoenrichment method enables a comprehensive characterization of the phosphoproteome.

■ ASSOCIATED CONTENT

Ⓢ Supporting Information

Method details and additional figures. This material is available free of charge via the Internet at http://pubs.acs.org.

■ AUTHOR INFORMATION

Corresponding Authors

*jin@chem.wisc.edu

*ge2@wisc.edu

Notes

The authors declare no competing financial interest.

■ ACKNOWLEDGMENTS

This work was supported by the NIH R21 EB013847 (to both S.J. and Y. G.). Y. G. also thanks the support by NIH R01 HL096971 and R01 HL109810. We would like to thank Ying-Hua Chang for critical reading of this manuscript and Yi Zhang for assistance in NPs synthesis.

■ REFERENCES

(1) Hunter, T. *Cell* **2000**, *100*, 113.

(2) (a) Tan, C. S. H.; Bodenmiller, B.; Pasculescu, A.; Jovanovic, M.; Hengartner, M. O.; Jørgensen, C.; Bader, G. D.; Aebersold, R.; Pawson, T.; Linding, R. *Sci. Signal.* **2009**, *2*, ra39. (b) Zhang, J.; Guy, M. J.; Norman, H. S.; Chen, Y.-C.; Xu, Q.; Dong, X.; Guner, H.; Wang, S.; Kohmoto, T.; Young, K. H.; Moss, R. L.; Ge, Y. *J. Proteome Res.* **2011**, *10*, 4054. (c) Huang, P. H.; Mukasa, A.; Bonavia, R.; Flynn, R. A.; Brewer, Z. E.; Cavenee, W. K.; Furnari, F. B.; White, F. M. *Proc. Natl. Acad. Sci. U. S. A.* **2007**, *104*, 12867.

(3) Nita-Lazar, A.; Saito-Benz, H.; White, F. M. *Proteomics* **2008**, *8*, 4433.

(4) (a) Mann, M.; Ong, S.-E.; Grønborg, M.; Steen, H.; Jensen, O. N.; Pandey, A. *Trends Biotechnol.* **2002**, *20*, 261. (b) Zhou, H.; Watts, J. D.; Aebersold, R. *Nat. Biotechnol.* **2001**, *19*, 375.

(5) (a) Tao, W. A.; Wollscheid, B.; O'Brien, R.; Eng, J. K.; Li, X.-j.; Bodenmiller, B.; Watts, J. D.; Hood, L.; Aebersold, R. *Nat. Methods* **2005**, *2*, 591. (b) Bodenmiller, B.; Mueller, L. N.; Mueller, M.; Domon, B.; Aebersold, R. *Nat. Methods* **2007**, *4*, 231. (c) Nelson, C. A.; Szczech, J. R.; Dooley, C. J.; Xu, Q.; Lawrence, M. J.; Zhu, H.; Jin, S.; Ge, Y. *Anal. Chem.* **2010**, *82*, 7193. (d) Nelson, C. A.; Szczech, J. R.; Xu, Q.; Lawrence, M. J.; Jin, S.; Ge, Y. *Chem. Commun.* **2009**, 6607.

(6) (a) Siuti, N.; Kelleher, N. L. *Nat. Methods* **2007**, *4*, 817. (b) Ge, Y.; Rybakova, I. N.; Xu, Q.; Moss, R. L. *Proc. Natl. Acad. Sci.U. S. A.* **2009**, *106*, 12658.

(7) (a) Schmidt, S. R.; Schweikart, F.; Andersson, M. E. *J. Chromatogr., B* **2007**, *849*, 154. (b) Oda, Y.; Nagasu, T.; Chait, B. T. *Nat. Biotechnol.* **2001**, *19*, 379. (c) Porath, J.; Carlsson, J. A. N.; Olsson, I.; Belfrage, G. *Nature* **1975**, *258*, 598.

(8) Kaur-Atwal, G.; Weston, D. J.; Bonner, P. L. R.; Crosland, S.; Green, P. S.; Creaser, C. S. *Curr. Anal. Chem.* **2008**, *4*, 127.

(9) (a) Rosi, N. L.; Mirkin, C. A. *Chem. Rev.* **2005**, *105*, 1547. (b) Gao, J.; Gu, H.; Xu, B. *Acc. Chem. Res.* **2009**, *42*, 1097. (c) Pan, Y.; Du, X.; Zhao, F.; Xu, B. *Chem. Soc. Rev.* **2012**, *41*, 2912. (d) Pan, Y.; Long, M. J. C.; Lin, H.-C.; Hedstrom, L.; Xu, B. *Chem. Sci.* **2012**, *3*, 3495.

(10) Aubin-Tam, M.-E.; Hamad-Schifferli, K. *Biomed. Mater.* **2008**, *3*, 034001.

(11) Sun, S. *Adv. Mater.* **2006**, *18*, 393.

(12) (a) Kinoshita, E.; Kinoshita-Kikuta, E.; Takiyama, K.; Koike, T. *Mol. Cell. Proteomics* **2006**, *5*, 749. (b) Kinoshita, E.; Kinoshita-Kikuta, E.; Koike, T. *Nat. Protoc.* **2009**, *4*, 1513. (c) Kinoshita, E.; Kinoshita-Kikuta, E. *Proteomics* **2011**, *11*, 319.

(13) Sun, S.; Zeng, H.; Robinson, D. B.; Raoux, S.; Rice, P. M.; Wang, S. X.; Li, G. *J. Am. Chem. Soc.* **2003**, *126*, 273.

(14) (a) De Palma, R.; Peeters, S.; Van Bael, M. J.; Van den Rul, H.; Bonroy, K.; Laureyn, W.; Mullens, J.; Borghs, G.; Maes, G. *Chem. Mater.* **2007**, *19*, 1821. (b) Jana, N. R.; Earhart, C.; Ying, J. Y. *Chem. Mater.* **2007**, *19*, 5074.

(15) Karakoti, A. S.; Das, S.; Thevuthasan, S.; Seal, S. *Angew. Chem., Int. Ed.* **2011**, *50*, 1980.

(16) Ojida, A.; Honda, K.; Shinmi, D.; Kiyonaka, S.; Mori, Y.; Hamachi, I. *J. Am. Chem. Soc.* **2006**, *128*, 10452.

(17) Trompeter, H.-I.; Blankenburg, G.; Brügger, B.; Menne, J.; Schiermeyer, A.; Scholz, M.; Söling, H.-D. *J. Biol. Chem.* **1996**, *271*, 1187.

(18) (a) Compton, P. D.; Zamdborg, L.; Thomas, P. M.; Kelleher, N. L. *Anal. Chem.* **2011**, *83*, 6868. (b) Xiu, L.; Valeja, S. G.; Alpert, A. J.; Jin, S.; Ge, Y. *Anal. Chem.* **2014**, *86*, 7899.

(19) Mammen, M.; Choi, S.-K.; Whitesides, G. M. *Angew. Chem., Int. Ed.* **1998**, *37*, 2754.

DOI: 10.1021/ja511833y
J. Am. Chem. Soc. 2015, 137, 2432−2435